EXPERIMENTAL INVESTIGATION OF THE GROWTH OF AN ISOLATED CRACK

V. M. Kuznetsov, P. A. Martynyuk, and A. I. Potylitsyn

Zhurnal Prikladnoi Mekhaniki i Tekhnicheskoi Fiziki, Vol. 10, No. 4, pp. 155–160, 1969

The results are presented of an experimental investigation of the growth of an isolated crack.

Using photoelastic analysis and high-speed motion photography, we determined the time dependence of the crack length and crack propagation rate. In contrast to the work of Wells and Post [5], we carried out a detailed analysis of the initial stages of crack propagation. With the aid of strain gauges we determined the time dependence of applied tensile stress; the results obtained are quite satisfactorily described by the formula postulated in [6].

Theoretical studies of non-steady-state propagation of an isolated crack during brittle fracture were carried out by Mott [1], Roberts and Wells [2], Broberg [3], and Barenblatt et al. [4]. Among experimental investigations, that carried out by Wells and Post [5] is worth mentioning.

Our experimental method was similar to that used in [5] in which the stress field in the vicinity of a crack growing in a plate specimen was studied. The motion-picture photographs of the process were taken with short exposures using four successive spark pulses. Wells and Post succeeded in obtaining only three points of the graph representing the dependence of the crack-propagation rate on crack length; these points were obtained only for the crack-propagation stage in which the crack-propagation rate almost reaches its limiting value, equal in this case to 0.38 of the velocity of elastic waves.

This made it possible for the authors of [4] to regard the crack-propagation rate as generally constant and to use Broberg's results obtained in solving a precisely formulated dynamic problem of the crack propagation from the state of rest at a constant velocity.

The optical part of the investigation carried out by Wells and Post was outstandingly good, photoelastic analysis being used to obtain detailed data on the stress state in the vicinity of the tip of a growing crack. The shortcomings of this work were the lack of control of forces applied to the specimen and the failure to obtain data on the initial crack propagation stages. One of the objects of the investigation described below was to eliminate these shortcomings.

1. Tensile testing machine. Ordinary tensile testing machines are so constructed that the load acting on a specimen increases gradually with increasing strain. In our case, to obtain data easy to interpret, it was necessary for a suddenly applied load to remain constant during the entire process of crack propagation or at least during a substantial part of this period. A special tensile testing machine was therefore designed for this purpose by V. N. Chertakov (Institute of Hydrodynamics, SO AN SSSR). Its general view is shown in Fig. 1; its design and principle of operation are described below.

The machine consists of a base plate 1 supporting two columns 2 braced at the top by a cross-bar 3. The ends of the columns are threaded to take nuts 4 with which the columns are fastened to the cross-bar and to the base plate.

The specimen is mounted in two shackles. The upper shackle 5 can be moved vertically by means of the nut 7 for accomodating specimens of different lengths and for preliminary selection of free play in the linkage of the loading unit. The lower shackle 6 with a movable crosspiece 8, helical spring 9, and cocking device 10 constitutes an independent loading unit.

The entire loading unit can be moved vertically so that the expected line of fracture can be positioned in the field of view of the recording apparatus. The loading unit has a separate force-generating system activated by spring 9. One end of the spring rests in a recess of the movable crosspiece 8 and the other end bears on plate 11, which is held in position by nut 12 screwed on the stem of the lower shackle 6. The force to be transmitted to the shackles is regulated by turning nut 12, i.e., by compressing spring 9. For transmitting the force of the spring to the specimen cocking and trigger mechanisms are provided.

These mechanisms form an integral part of the force-generating system which is linked to the movable crosspiece

and which includes the lower shackle 6 with its threaded stem; a hole is milled in the end of the stem for attaching the two-arm cocking mechanism 13. The cocking and trigger mechanism 10 constitutes a rigid frame, in the opposite vertical walls of which screw 14 for cocking spring 9 and trigger rod 15 with a releasing lever 16 are mounted.

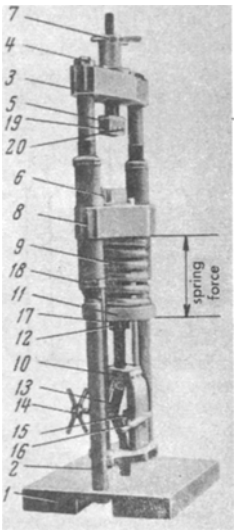

Fig. 1

The two-arm mechanism 13 constitutes two plates connected by a hinged joint. Its upper end is linked through a connecting rod to the stem of the lower shackle 6 and its lower end is hinged on the inside surface of the base of the frame of the trigger device. When the loading system is cocked, the force-generating system is closed by securing it to the movable crosspiece 8 with pins 17; to prevent deviation of the system from coaxiality, a cylindrical stem free to move in a corresponding hole in the base plate 1 is attached to the lower part of the frame of the cocking-triggering device.

To soften the impact of the lower shackle striking the movable crosspiece when the specimen breaks, a cylindrical recess is made in the crosspiece; a rubber washer covered by a metal plate is placed in this recess. In this way the impact of the lower shackle is softened by the rubber shock absorber. To make it possible to position the shackles in accordance with the specimen length and keep the line of fracture in the same plane, a provision was made for moving the crosspiece 8 in the vertical direction with the aid of nuts 18; at the same time the loading and cocking-triggering devices, which are attached to the crosspiece, are also moved. The specimen is secured in the shackles with the aid of sponge pads 19 and bolts 20. The load applied to the specimen can be preset at any level in the range 0–2000 kg by tightening nut 12 on the stem of the lower shackle.

2. Experimental technique. The tests were carried out on organic glass plate specimens measuring 220 × 110 × 3 mm. Before testing, an artificial crack 3–4 mm long was made in each specimen. The photographs were taken in a polarized light with the aid of an SFR-2M photorecorder at a speed of 250,000 frames/sec.

A schematic representation of the apparatus is shown in Fig. 2. Here 1 is the control panel, 2 is an IFK-2000 pulse lamp with a reflector, 3 is a discharger, 4 is a battery of condensers for fusing the wire, 5 is a battery of condensers of the pulse lamp, 6 is a delay block, 7 is a pulse generator, 8 is the SFR-2M, 9 is the testing machine with a specimen, 10 is a lens, and 11 and 12 are polaroids.

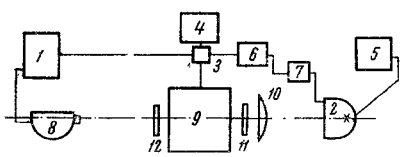

Fig. 2

The main difficulty was encountered in synchronizing the onset of crack propagation with the starting of the photorecorder. Preliminary tests showed that the time interval between starting the testing machine and the onset of crack propagation is 2.2–2.6 msec.

In addition, it was necessary to synchronize the onset of crack propagation with the initial positioning of the photorecorder mirror and with the flash of the illuminating lamp.

The testing machine was therefore started in the following way. The trigger mechanism of the spring 13 was bearing on a plexiglass rod (Fig. 3) with a 0.2-mm copper wire inside it. This wire was in the circuit of the battery of condensers; when it was blasted, the rod desintegrated, which activated the trigger mechanism of the testing machine.

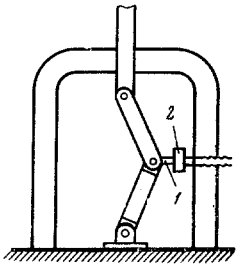

Fig. 3

The electrical circuit of the apparatus is shown in Fig. 4. When the photogenerator is started, it emits a high-voltage pulse through the discharger 3, by which the battery of condensers 4 (12 μF, 25 kV) is connected to the wire 8 inside the plexiglas rod and to the pulse generator 7 and pulse flash-lamp 2 (IFK-2000) through the delay block 6. The diagram in Fig. 4 shows the following components: 1) control panel; 2) IFK-2000 pulse lamp; 3) discharger; 4) battery of 12-μF/25-kV condensers; 5) battery of condensers (800 μF/1.0 kV) of the pulse lamp; 6) delay block; 7) pulse generator; 8) plexiglas rod with a copper wire; 9) charging device Tesla VS-222; 10) charging device UPU-1M.

The results of special experiments showed that the time interval between pushing the starting button on the control panel 1, i.e., starting the disintegration of the plexiglas rod, and the onset of crack propagation is of the order of 2.5 msec ± 200 μsec. On this basis, the delay block 6 switched on the flash lamp 2 slightly before the onset of crack propagation; the advance was 100–150 μsec, the flash duration being 450–500 μsec.

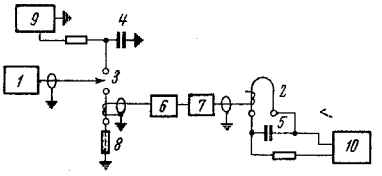

Fig. 4

The initial setting of the angle of the photorecorder mirror was selected on the basis of the same considerations, so that the advance was 2.5 msec. By varying the length of the plexiglas rod it is possible to vary within known limits the delay time in starting the machine. Polaroids 11 and 12 were used mainly to mark more clearly the position of the crack tip.

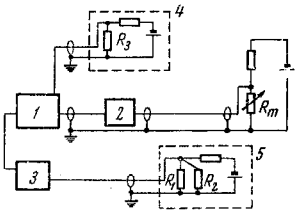

Fig. 5

In addition to taking motion pictures of the crack propagation, measurements of stresses in the specimen were carried out. This was done with the aid of the PKB5-100 strain gauges attached to the specimen.

The electric circuit of the strain measuring system is shown in Fig. 5. It comprises the following components: 1) OK-17M oscillograph; 2) cathodic repeater; 3) G5-15 pulse generator; 4) oscillograph recorder circuit; 5) pulse

generator triggering circuit (R_1 and R_2 corresponding to the beginning and end of crack propagation, respectively); R_1 and R_3 are resistances of conducting films (of the order of 3-5 kohms) deposited on the specimen; R_m is the strain gauge.

Signals from the strain gauge were transmitted to one beam of the OK-17M oscillograph through the cathodic repeater, the amplification coefficient of the cathodic repeater/amplifier system being of the order of $4 \cdot 10^4$. The other beam was used to mark the instants of the onset of crack propagation and its reaching the free specimen surface The signals of the beginning and end of crack propagation were produced as a result of breaking of conducting films deposited on the specimen in front of the tip of the initial crack and near the opposite side of the specimen.

3. Experimental results. Motion-picture frames showing successive stages of crack propagation are reproduced in Fig. 6. The time intervals between frames were 8 μsec. The results of the processing of experimental data are shown in Fig. 7, where the crack length (curve 1) and crack propagation rate (curve 2) are plotted against time. The character of the time dependence of the tensile stress as recorded by the oscillograph (curve 1) and the strain-gauge calibration curve (curve 2) are shown in Fig. 8. Each step on the calibration curve corresponds to a 200-kg increase in applied load. The sharp reduction in stress is associated with the strain gauge being influenced by an unloading wave arriving at it from the crack and by the wave reflected from the unbroken edge of the specimen.

4. Analysis of the results. The Mott formula in its more precise form derived by Roberts and Wells is

$$V = 0.38\left[\frac{E}{\rho}\left(1-\frac{l_0}{l}\right)\right]^{1/2} \tag{1}$$

Here l_0 is the initial crack length and l is the crack length at a given propagation stage. The formula postulated in [6] has the form

$$V = c_0\left[1-\left(\frac{l_0^*}{l}\right)^{1/2}\right]^{1/2} \tag{2}$$

Here c_0 is the velocity of the Rayleigh waves and l_0^* is the length of a crack in a state of equilibrium at a given tensile stress. It should be noted that the difference between these two formulas consists not only in a small difference between their constants and between the form of the functional relationship, but also in different meanings of l_0. In accordance with the generally accepted tenets of the theory of brittle fracture [7, 14], the equilibrium crack length is related to tensile stress p by the Griffith formula, which, in the case of a crack emerging on the boundary of a half-space, has the form [8]

$$l_0^* = 1.61\frac{K^2}{p^2} \tag{3}$$

where K is the cohesion modulus.

The length of an equilibrium crack l_0° corresponding to the static tensile strength σ_* of the material is given by a similar formula:

$$l_0^\circ = 1.61\frac{K^2}{\sigma_*^2} \tag{4}$$

Thus, the equilibrium crack length at stresses exceeding the material strength is shorter than under static loading conditions:

$$l_0^* = l_0^\circ\left(\frac{\sigma_*}{p}\right)^2 \tag{5}$$

At the same time, the crack length l_0° is determined by the ratio of the theoretical and actual material strength [9], and its order of magnitude in the case of a purely brittle fracture mechanism is given by

$$l_0^\circ \sim 10b\left(\frac{\sigma_T}{\sigma_*}\right)^2$$

Here $b \sim 10^{-8}$ cm is the interatomic spacing and σ_T is the theoretical strength, approximately equal to 0.1 E (where E is the Young modulus). According to data cited in reference books [10] the tensile strength of thermoplastic

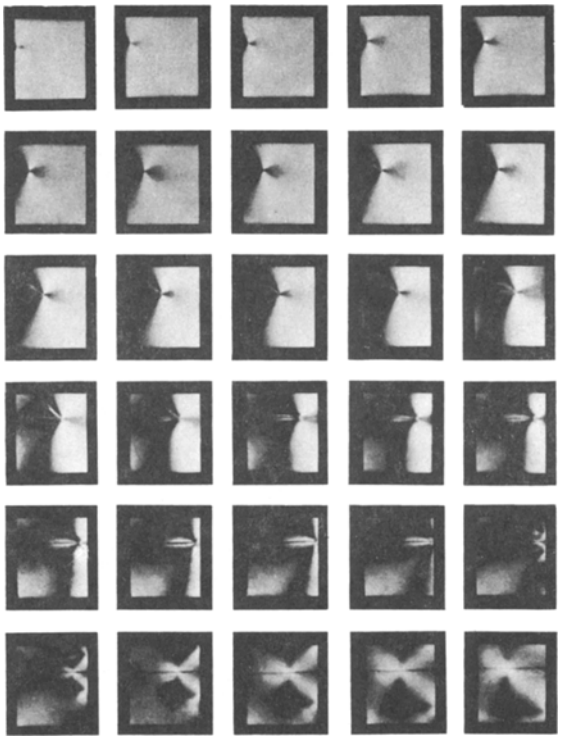

Fig. 6

plastics, which include plexiglas, is $(0.28-0.70) \cdot 10^9$ dynes/cm^2 and their Young's modulus is $(0.14-0.28) \cdot 10^{11}$ dynes/cm^2. Thus, we find that l_0° is very small, of the order of $(0.2-1.0) \cdot 10^{-6}$ cm. However, the above calculation contains a serious error. The point is that a substantial part in the crack propagation in most materials is played by local plastic strains concentrated in thin surface layers of the crack.

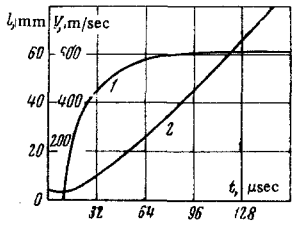

Fig. 7

As shown by Irwin [11] and Orowan [12], the work of plastic deformation during quasi-brittle fracture can be, by several orders of magnitude, larger than the usual coefficient of surface tension, which is equal to specific work expended in rupturing internal bonds.

The effective magnitude of surface tension determined from the results of experiments on cleavage fracture of plexiglas specimens is 12,000 cal/cm^2, which corresponds to a cohesion modulus of 150 cal/cm^2. The tensile strength of the plastic used in our experiments was 500 ± 50 kg/cm^2; its Young's modulus E = $1.8 \cdot 10^4$ kg/cm^2 and density ρ = = 1.13 g/cm^3. According to the data in [13], the velocity of longitudinal waves in plastic is 2800 m/sec. Using the known relations for the velocities of longitudinal (c_1) and transverse (c_2) waves

$$c_1 = \left[\frac{E}{\rho}\frac{1-\nu}{(1+\nu)(1-2\nu)}\right]^{1/2}, \quad c_2 = \left[\frac{E}{\rho}\frac{1}{2(1+\nu)}\right]^{1/2}$$

we obtain the Poisson's ratio ν = 0.435 and c_2 = 900 m/sec. The velocity of Rayleigh waves is approximately equal to $0.9c_2$. Thus, in our case it may be assumed that c_0 = 800 m/sec. In the case of plate specimens undergoing deformation we are dealing with a plane stress state, so that the cohesion modulus should be calculated from the formula $K_1 = K\sqrt{1-\nu^2}$. Instead of 150 kg/cm^2 one should therefore take 135 kg/cm^2. Substituting into (4) the values of K and σ_*, we obtain l_0° = 1.1 mm.

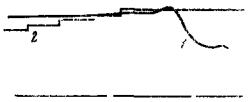

Fig. 8

To determine l_0^* from (5) the tensile stress must be known. As shown by the oscillogram in Fig. 8, p varies with time. To simplify the calculations, it is assumed that p remains constant at a certain mean level. According to the oscillogram in Fig. 8, the over-all tensile load varies between 600 and 950 kg. Let the mean load level be 775 kg. Since the plate specimen is 11 cm wide and 0.3 cm thick, this is equivalent to p = 235 kg/cm^2. From (5) we have l_0^* = 5 mm.

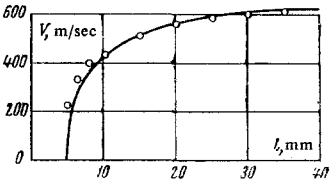

Fig. 9

In Fig. 9 we plotted Eq. (2) taking c_0 = 800 m/sec and l_0^* = 5 mm; in the same figure we plotted experimental points obtained from motion picture frames in Fig. 6 and the graph in Fig. 7. The agreement between experimental and calculated data is quite satisfactory.

REFERENCES

1. N. F. Mott, "Fracture of metals; theoretical considerations," Engineering, vol. 165, pp. 16–18, 1948.

2. D. K. Roberts and A. A. Wells, "The velocity of brittle fractures," Engineering, vol. 178, pp. 820–821, 1954.

3. K. B. Broberg, "The propagation of a brittle crack," Arkiv fys., vol. 18, pp. 159–192, 1960.

4. G. I. Barenblatt, R. L. Salganik, and G. P. Cherepanov, "Non-steady-state crack propagation," PMM, vol. 26, no. 2, 1962.

5. A. A. Wells and D. Post, "The dynamic stress distribution surrounding a running crack—a photoelastic analysis," Proc. Exper. Stress Analysis, vol. 16, no. 1, 1958.

6. V. M. Kuznetsov, "Non-steady-state propagation of a system of cracks in brittle materials," PMTF [Journal of Applied Mechanics and Technical Physics], no. 2, 1968.

7. G. I. Barenblatt, "Mathematical theory of equilibrium cracks formed during brittle fracture," PMTF, no. 4, 1961.

8. G. R. Irwin, "The crack extension force for a crack at a free surface boundary," NRh Rept., no. 5120, 1958.

9. Atomic Mechanism of Fracture [in Russian], Metallurgizdat, Moscow, 1963.

10. G. W. C. Kaye and T. H. Laby, Tables of Physical and Chemical Constants [Russian translation], Fizmatgiz, Moscow, 1962.

11. G. R. Irwin, "Fracture dynamics," in: Fracture of Metals, ASM, Cleveland, pp. 147–166, 1948.

12. E. O. Orowan, "Fundamentals of brittle behavior of metals," in: Fatigue and Fracture of Metals, Wiley, N. Y., pp. 139–167, 1950.

13. V. V. Adushkin and P. O. Sukhotin, "Explosive fracture of solids," PMTF, no. 4, 1961.

14. G. R. Irwin, in: Handbuch der Physik, Vol. 4, Springer, Berlin, pp. 551–558, 1958.

23 December 1968

Novosibirsk